JOURNAL OF CATALYSIS 128, 23–33 (1991)

Microcalorimetric Measurements of Basic Molecule Adsorption on Silica and Silica–Alumina

NELSON CARDONA-MARTÍNEZ[1] AND J. A. DUMESIC[2]

Department of Chemical Engineering, University of Wisconsin, Madison, Wisconsin 53706

Received May 30, 1990; revised October 1, 1990

The differential heats of adsorption of ammonia, pyridine, trimethylamine, and triethylamine on silica–alumina and silica were determined microcalorimetrically to investigate how the heat of adsorption for a given site depends on the nature of the basic molecule adsorbed. This provides a test of the utility of the Drago–Wayland theory to heterogeneous reactions. Specifically, the acid/base properties of molecules in solution are described in terms of two parameters, the susceptibility of the species to undergo electrostatic interaction and the susceptibility to form covalent bonds. Accordingly, the calorimetric results of this study were correlated successfully in terms of Drago parameters for each catalyst. These parameters describe well the acidic properties of silica–alumina and silica and may allow the prediction of heats of adsorption for a wide range of basic molecules with known Drago parameters.

INTRODUCTION

In previous studies (*1*, *2*), we have used microcalorimetry to measure the differential heat of adsorption of pyridine on a series of silica–supported metal oxides. This work was carried out to formulate a thermodynamic scale of surface acidity for these materials. In the present study, we explore the dependence of the differential heat of adsorption on the nature of the base molecule used in microcalorimetric measurements of surface acidity.

The dependence of the differential heat of adsorption upon the nature of the adsorbed molecule is an area of research which has received little attention for solid acid catalysts. The acid/base properties of molecules in solution can be described typically in terms of two parameters (3), the susceptibility of the species to undergo electrostatic interactions, E, and the susceptibility to form covalent bonds, C, as shown below:

$$\Delta H = E_A E_B + C_A C_B. \quad (1)$$

These parameters define the Drago–Wayland scale and they are tabulated for many molecules in the literature (*4*, *5*). In the present paper we test the viability of acid strength prediction for different basic molecules by correlation of the heat of adsorption of selected probe molecules on silica and silica–alumina in terms of two corresponding parameters for the acid sites that exist on these oxides. If this approach can be extended to other systems, it would be possible to predict the heat of adsorption of a variety of molecules on surface acid sites.

To incroporate a new acid (or base) to the Drago–Wayland scale, the interaction of that molecule with a series of bases (or acids) with known E and C parameters must be studied. The most important criteria to select these bases are that they have widely differing C/E ratios and that steric effects are absent. When the molecules have similar C/E ratios, the determined Drago/Wayland parameters will be poorly defined even though a good fit of the data is possible. Ammonia, pyridine, triethylamine, and trimethylamine were chosen because their

[1] Present address: University of Puerto Rico, Chemical Engineering Department, P.O. Box 5000, Mayagüez, P.R. 00709-5000

[2] To whom correspondence should be addressed.

0021-9517/91 $3.00

TABLE 1

Properties of Selected Probe Base Molecules[a]

Probe molecule	C_B (kJ mol^{-1})$^{0.5}$	E_B (kJ mol^{-1})$^{0.5}$	$\frac{C_B}{E_B}$	PA (kJ mol^{-1})	vIP (kJ mol^{-1})	pK_a
NH_3	7.08	2.78	2.54	857.7	1046.8	9.3
PYR	13.10	2.39	5.48	922.2	926.3	5.2
TEA	22.59	2.03	11.12	967.3	774.9	10.8
TMA	23.61	1.65	14.30	938.5	823.0	9.8

[a] C_B and E_B Drago–Wayland parameters from Ref. (*4*). PA, proton affinity: the negative of the enthalpy for

$$Base_{(g)} + H^+_{(g)} \leftrightarrows BaseH^+_{(g)} \quad PA = -\Delta H$$ from Ref. (*32*).

vIP, vertical ionization potential: the amount of energy (in eV) necessary to remove an electron from the molecule in the gas phase; from Ref. (*32*). pK_a from Refs. (*23, 33*).

C/E ratios are considerably different, as shown in Table 1, and because these bases have been used in previous microcalorimetric studies.

Drago–Wayland parameters have not been determined for mixed oxides. A review of the literature indicates that this approach has been used to estimate these parameters for a few solid surfaces. Fowkes and co-workers (*6–9*) calculated C_A and E_A values for SiO_2, TiO_2, and Fe_2O_3 using a combination of UV and IR spectroscopies and a flow calorimeter. They determined heats of adsorption of pyridine, triethylamine, ethyl acetate, acetone, and polymethylmethacrylate (PMMA) in neutral hydrocarbon solutions. However, their results did not provide consistent *C/E* parameters for the surface acid sites. It should be noted that the heats determined were for high surface coverages and these values provide a lower bound for the actual acid strength distribution.

Lim *et al.* (*10*) determined heats of adsorption of pyridine, *n*-methylimidazole, and dimethylcyanamide from cyclohexane solution onto PdO crystallites supported on carbon using a procedure similar to the one above. A large set of E_A and C_A parameters was found to fit the data. The heats determined were isosteric and there was a significant contribution from the support, which complicated the interpretation of the data.

Silica and silica–alumina have been previously studied with microcalorimetry. The differential heat of ammonia adsorption on silica has been determined for a wide range of temperatures by various authors (*11–14*). Initial differential heats from 53 to 85 kJ mol^{-1} have been reported. The acid strength distribution plots for silica do not show maxima, the differential heat decreasing slowly, almost linearly with coverage.

The adsorption of triethylamine on a hydroxylated aerosilogel has been studied from 294 to 486 K up to coverages of 400 μmol g^{-1} by Derkaui and co-workers (*15, 16*). These authors reported initial differential heats from 100 to 110 kJ mol^{-1}, and their acid strength distribution plots at temperatures lower than 409 K showed maxima between 75 and 82 kJ mol^{-1}. The differential heat decreased linearly at higher temperatures, and the amount adsorbed decreased appreciably.

Curthoys *et al.* (*17*) studied the adsorption of triethylamine and pyridine on silica with an isoperibol calorimeter. The initial differential heats were 92 and 94 kJ mol^{-1}, respectively, for triethylamine and pryidine. The acid strength distribution plot for triethylamine showed a maximum at 84 kJ mol^{-1}, and the plot for pyridine had a peak near 75 kJ mol^{-1}.

The differential heat of adsorption of ammonia on silica–alumina with different Al

loadings has also been determined for a wide range of temperatures by various authors (*11–14, 18–21*). The reported initial differential heats vary from 125 to 170 kJ mol^{-1}. The acid strength distribution plots for silica–alumina displayed maxima between 105 and 120 kJ mol^{-1}.

EXPERIMENTAL PROCEDURE

Samples were prepared and pretreated as described elsewhere (*1, 2*). The ammonia and trimethylamine gases used were of high purity (99.99% and 99%+, respectively) from Matheson Gas Products (Chicago). The pyridine and triethylamine liquids used were high-purity materials (Gold Label 99%+) from Aldrich Chemicals (Milwaukee). The basic probe molecules were dried by storage over activated molecular sieve (3A) and purified with the freeze–pump–thaw technique before each run. The experimental procedure and microcalorimetry apparatus have been described previously (*1, 22*), with the exception that the dosing volume was maintained at a higher temperature (318–323 K). The basic probe molecules were kept in a constant temperature bath to control the vapor pressure between 500 and 5000 Pa (*23–25*).

RESULTS/DISCUSSION

Pyridine Adsorption

Microcalorimetric results for pyridine adsorption on silica at 473 K have been discussed in a previous publication (*1*). Briefly, it was found that the silica surface is energetically homogeneous for the extents of coverage studied, giving an approximately constant differential heat of adsorption of 95 kJ mol^{-1} and an entropy change of adsorption of -167 J mol^{-1} K^{-1}. The differential heat determined is considerably higher than the heat of condensation of pyridine, 35.1 kJ mol^{-1} (*23*) and compares favorably with the initial differential heat of adsorption of 94 kJ mol^{-1} reported by Kiselev and co-workers (*17*) for the adsorption of pyridine on a macroporous silica–aerosilogel after evacuation at 473 K. Using statistical mechanics and

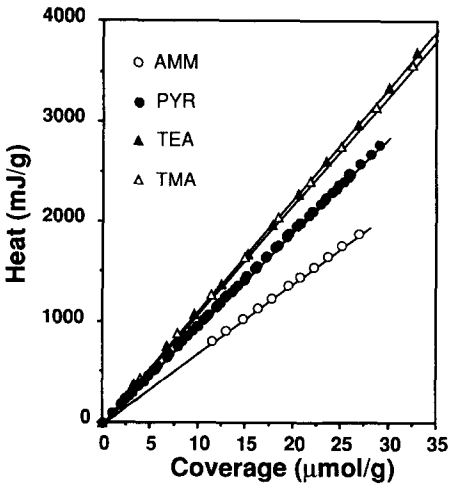

FIG. 1. Integral heat of basic molecule adsorption on silica (○ ammonia adsorbed at 423 K, ● pyridine adsorbed at 473 K, ▲ triethylamine adsorbed at 473 K, △ trimethylamine adsorbed at 423 K, —— fit).

the volumetric adsorption data we estimated an activation energy for surface diffusion of approximately 20 kJ mol^{-1}, which indicates that under these conditions pyridine retains a significant fraction of its mobility. This result is consistent with ^{13}C NMR spectroscopy which indicated that pyridine adsorbed on silica is in a state of rapid motion even at 301 K (*26*). The results for pyridine adsorption on silica are included in Fig. 1.

The results for pyridine adsorption on silica-supported aluminum oxide at 473 K were also discussed previously (*1*). In short, depositing alumina on SiO_2 increased the acidity of the catalyst considerably. The differential heat of adsorption for pyridine adsorbed silica-supported aluminum oxide at 473 K is included in Fig. 2. The initial differential heat of pyridine adsorption was determined to be 219 kJ mol^{-1}. Adsorption at 473 K yields three regions of nearly constant heats of adsorption with an intermediate step near 170 kJ mol^{-1}. The experimental integral heat data were fit using a Langmuir model for three sites as described in Ref. (*1*). To obtain this fit, as well as other fits in this work, the values found for silica were assigned to the energetically weakest

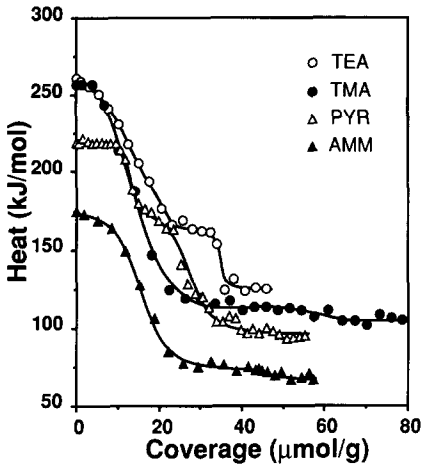

FIG. 2. Average differential heat, $\{\Delta Q/\Delta n\}_i$, of basic molecule adsorption on Al_2O_3/SiO_2 (○ triethylamine adsorbed at 473 K, ● trimethylamine adsorbed at 423 K, △ pyridine adsorbed at 473 K, ▲ ammonia adsorbed at 423 K, —— fit).

site or allowed to vary near those values. A summary of the results for adsorption on Al_2O_3/SiO_2 at 473 K is presented in Table 2.

Ammonia Adsorption on Silica

Ammonia was the weakest base studied in this work. The ammonia reservoir was kept at 195 K to control the vapor pressure at approximately 4.9 kPa.

The integral heat of ammonia adsorption on silica at 423 K as a function of surface coverage is shown in Fig. 1. An adsorption temperature lower than that for pyridine measurements was used to decrease the possibility of dissociative adsorption. Since desorption from the dosing volume walls caused experimental errors in the average differential heat for low coverages, the values for coverages higher than 10 μmol g^{-1} were used to determine the differential heat of adsorption; and the plot of the integral heat of adsorption was adjusted to intersect the axes at zero. Using least-squares we calculate a differential heat of 70 kJ mol^{-1}. Such a heat is considerably higher than the heat of condensation of ammonia at room temperature, 21.7 kJ mol^{-1} (*24*). The heat of condensation at 423 K is zero because this temperature is higher than the critical temperature (405.6 K). The heat determined in this study compares favorably with the initial differential heat of adsorption of approximately 70 kJ mol^{-1} reported by Auroux and Védrine (*14*) for the adsorption of ammonia on fumed silica at 300 K after evac-

TABLE 2

Parameters for Fit of Integral Heat of Pyridine Adsorption on Al_2O_3/SiO_2 at 473 K with the Langmuir Model for Three Sites

Probe molecule	Adsorption temperature (K)	Site i	$n_{m,i}$ (μmol g^{-1})	$q_{initial}$ (kJ mol^{-1})	ΔS_i (J mol^{-1} K^{-1})
Pyridine	473	1	12.7	220	−330
		2	14.8	177	−289
		3	140	96	−165
Ammonia	423	1	12	181	−330
		2	13	100	−167
		3	140	69	−132
Trimethylamine	423	1	12	267	−530
		2	13	164	−318
		3	140	103	−191
Triethylamine	473	1	12	270	−486
		2	13	170	−269
		3	140	112	−183

uation at 323 K; however, our value is different than the heat of ammonia adsorption on a precipitated silica (≈85 kJ mol^{-1}) studied by these authors at the same conditions. Our silica is a fumed silica.

The ammonia adsorption isotherm on silica at 423 K was fit to a Langmuir isotherm with an equilibrium constant K. In this fit, the monolayer coverage was fixed at the value found for pyridine adsorption (140 μmol g^{-1}) (*1*). This was done since we did not study the adsorption of ammonia at high surface coverages, and the fitted value of the monolayer coverage is not well defined. By fixing it at the value found for pyridine, which was studied in more detail, we establish an upper bound for the calculated change in entropy of adsorption. The adsorption of ammonia on silica at 423 K can be described with the following parameters:

$$K = 3.5 \times 10^{-4} \pm 5 \times 10^{-5}\ \mathrm{Pa}^{-1}$$
$$n_m = 140\ \mu\mathrm{mol\ g}^{-1}$$
$$q = 69.9 \pm 0.6\ \mathrm{kJ\ mol}^{-1}$$
$$\Delta S_{ads} = -135 \pm 1\ \mathrm{J\ mol}^{-1}\ \mathrm{K}^{-1}.$$

The gas phase entropy of ammonia at 423 K is 205.3 J mol^{-1} K^{-1} (*24*). Using partition functions and the structural and vibrational data given in (*24*), the estimates for the translational, rotational, and vibrational contributions to the gas phase entropy are

$$S_t = 147.7\ \mathrm{J\ mol}^{-1}\ \mathrm{K}^{-1},$$
$$S_r = 52.6\ \mathrm{J\ mol}^{-1}\ \mathrm{K}^{-1},$$
$$S_v = 3.1\ \mathrm{J\ mol}^{-1}\ \mathrm{K}^{-1}.$$

The estimated entropy changes of adsorption correspond to a loss of about 66% of the ammonia gas phase entropy. This magnitude is less than the translational contribution to the gas phase entropy. Using the same procedure for pyridine adsorption on silica discussed in Ref. (*1*), it can be estimated that adsorption of ammonia corresponds to an 84% loss of translational freedom and a 34% loss of rotational freedom along the *x* and *y* axes parallel to the surface. Thus, ammonia adsorbed on silica at 423 K appears to be as mobile as pyridine at 473 K. This result is consistent with ammonia being a weaker gaseous base than pyridine. As a result, we can expect silica to facilitate the equilibration of ammonia among strong sites on the surface better than for the case of pyridine adsorption at 473 K, and we can expect true site distributions even on catalysts with strong sites. Using the same approach used in Ref. (*1*) the maximum differential heat at which we should expect equilibration of ammonia on the surface is about 190 kJ mol^{-1}.

Ammonia Adsorption on Aluminum Supported on Silica

The loading of the Al specimens used in this work, except for pyridine adsorption, was 0.23 wt% Al, which corresponds to 1.29×10^{17} cations m^{-2}. The curve of the differential heat of adsorption of ammonia on Al_2O_3/SiO_2 at 423 K is shown in Fig. 2. The initial differential heat of ammonia adsorption on Al_2O_3/SiO_2 is calculated to be 176 kJ mol^{-1} from the slope at zero coverage of the integral heat curve. The plot of differential heat of ammonia adsorption on Al_2O_3/SiO_2 does not display an intermediate step like the one seen for pyridine adsorption. The parameters found after fitting the integral heat data and the adsorption isotherm with the Langmuir model are given in Table 2. In this fit the full coverages for sites 1 and 2 were constrained to values within 10% (after correcting for the difference in loading) of those found for pyridine adsorption. The value found for pyridine adsorption on silica was used for site 3. The order of the entropy changes for the three sites is reasonable in this fit. The entropy change for site 1, however, is higher than the ammonia gas phase entropy at 423 K indicating that ammonia is irreversibly adsorbed on these sites.

Trimethylamine Adsorption on Silica

Trimethylamine is a stronger base than pyridine. The trimethylamine reservoir was kept at 195 K to control the vapor pressure at approximately 1.0 kPa.

The integral heat of trimethylamine adsorption on silica at 423 K as a function of surface coverage is shown in Fig. 1. An adsorption temperature lower than that for pyridine was used to decrease the possibility of dissociative adsorption on the Al_2O_3/SiO_2 sample (*27*). Using least-squares, we calculate a differential heat of 109 kJ mol^{-1}. Such a heat is considerably higher than the heat of condensation of trimethylamine at room temperature, 22.9 kJ mol^{-1} (*24*). The critical temperature for trimethylamine is 433.2 K.

A constrained fit of the differential heat and adsorption isotherm data was carried out as described for ammonia, giving the following parameters for trimethylamine on silica:

$$K = 5.5 \times 10^{-3} \pm 3 \times 10^{-4}\ \text{Pa}^{-1}$$
$$n_m = 140\ \mu\text{mol g}^{-1}$$
$$q = 109.4 \pm 0.2\ \text{kJ mol}^{-1}$$
$$\Delta S_{ads} = -206 \pm 1\ \text{J mol}^{-1}\ \text{K}^{-1}.$$

The gas phase entropy of trimethylamine at 423 K is 327.1 J mol^{-1} K^{-1} (*24*). Using partition functions, and the structural parameters (*28*) and vibrational spectrum of trimethylamine (*29*), the estimates for the translational, rotational, and vibrational contributions to the gas phase entropy are

$$S_t = 163.3\ \text{J mol}^{-1}\ \text{K}^{-1},$$
$$S_r = 97.7\ \text{J mol}^{-1}\ \text{K}^{-1},$$
$$S_v = 64.0\ \text{J mol}^{-1}\ \text{K}^{-1}.$$

The estimated entropy change of adsorption corresponds to a loss of about 63% of the trimethylamine gas phase entropy. The magnitude of this change is higher than the translational contribution to the gas phase entropy. Using the same procedure for pyridine adsorption on silica discussed in Ref. (*1*), the above results represent a 92% loss of translational freedom and a 73% loss of rotational freedom along the x and y axes parallel to the surface. Thus, trimethylamine adsorbed on silica at 423 K loses most of its mobility. Therefore, we should not expect silica to facilitate the equilibration of trimethylamine among strong sites on the surface as much as pyridine and ammonia, and probably at low coverages, an average acid strength distribution will be obtained.

Trimethylamine Adsorption on Aluminum Supported on Silica

The curve of the differential heat of adsorption of trimethylamine on Al_2O_3/SiO_2 at 423 K is shown in Fig. 2. The initial differential heat of trimethylamine adsorption on Al_2O_3/SiO_2 is calculated as 257 kJ mol^{-1}. The shape of the plot of differential heat of trimethylamine adsorption is similar to the one determined for ammonia adsorption and does not display an intermediate step. There appears to be a step at higher coverages. Fitting the integral heat and volumetric data with the Langmuir model, constraining the monolayer coverages at the values used for ammonia, gives a good fit. The parameters found are given in Table 2.

The entropy change of adsorption for site 1 is considerably higher than the trimethylamine gas phase entropy, indicating irreversible adsorption or a surface reaction. The entropy change for site 2 represents about 97% of the gas phase entropy and also probably corresponds to irreversible adsorption. As a result, adsorption of trimethylamine of Al_2O_3/SiO_2 at 423 K is most probably nonspecific and the differential heats at low coverages probably are average values.

Triethylamine Adsorption on Silica

Triethylamine was the strongest base studied in this work. The triethylamine reservoir was kept at 263 K to control the vapor pressure at approximately 750 Pa.

Triethylamine was adsorbed on silica at 423 and 473 K to test the effect of adsorption temperature on the acid strength distribution. The integral heat of triethylamine adsorption on silica at 473 K as a function of surface coverage is shown in Fig. 1. The fitted differential heat was the same at both adsorption temperatures within experimental error, 112 kJ mol^{-1}. Such a heat is considerably higher than the heat of condensa-

tion of triethylamine at room temperature, 35.6 kJ mol^{-1} (*23*). The critical temperature for trimethylamine is 535 K. The fitted differential heat of adsorption, as well as the average differential heat for individual doses, are shown in Fig. 2.

A constrained fit of the differential heat and volumetric data at 423 K to a Langmuir model gives the following parameters:

$$K = 1.7 \times 10^{-2} \pm 1 \times 10^{-3}\ Pa^{-1}$$
$$n_m = 140\ \mu mol\ g^{-1}$$
$$q = 111.8 \pm 0.1\ kJ\ mol^{-1}$$
$$\Delta S_{ads} = -202 \pm 1\ J\ mol^{-1}\ K^{-1}.$$

The gas phase entropy of triethylamine at 423 K is 472.6 J mol^{-1} K^{-1} (*23*). Using partition functions and structural parameters for triethylamine (*30*), the estimates for the translational, rotational, and vibrational contributions to the gas phase entropy are:

$$S_t = 170.0\ J\ mol^{-1}\ K^{-1},$$
$$S_r = 112.8\ J\ mol^{-1}\ K^{-1},$$
$$S_v = 189.9\ J\ mol^{-1}\ K^{-1}.$$

Estimation of the vibrational contribution to the gas phase entropy for triethylamine is more difficult than that for the other molecules studied in this work because a large fraction of it corresponds to flopping motion and internal rotations that are difficult to assess quantitatively. The vibrational contribution was determined by subtracting the translational and rotational contributions from the experimentally determined gas phase entropy. The estimated entropy change of adsorption corresponds to a loss of about 43% of the ammonia gas phase entropy. This magnitude is larger than the translational contribution to the gas phase entropy. Using the same procedure for pyridine adsorption on silica discussed in Ref. (*1*), the adsorption entropy corresponds to a 58% loss of rotational freedom along x and y axes parallel to the surface and 90% loss of translational mobility.

Fitting the differential heat and adsorption isotherm data at 473 K leads to the following parameters:

$$K = 3.6 \times 10^{-3} \pm 2 \times 10^{-4}\ Pa^{-1}$$
$$n_m = 140\ \mu mol\ g^{-1}$$
$$q = 112 \pm 1\ kJ\ mol^{-1}$$
$$\Delta S_{ads} = -188 \pm 1\ J\ mol^{-1}\ K^{-1}.$$

The gas phase entropy of triethylamine at 473 K is 497.6 J mol^{-1} K^{-1}. Using partition functions, the estimates for the translational, rotational, and vibrational contributions to the gas phase entropy are:

$$S_t = 171.4\ J\ mol^{-1}\ K^{-1},$$
$$S_r = 114.2\ J\ mol^{-1}\ K^{-1},$$
$$S_v = 212.0\ J\ mol^{-1}\ K^{-1}.$$

The estimated entropy change of adsorption corresponds to a loss of about 38% of the triethylamine gas phase entropy. This magnitude is again larger than the translational contribution to the gas phase entropy. The calculated adsorption entropy corresponds to a 49% loss of rotational freedom along the x and y axes parallel to the surface and an 89% loss of translational freedom. Hence, increasing the adsorption temperature to 473 K yields a small increase in surface mobility.

Triethylamine Adsorption on Aluminum Supported on Silica

The curve of the differential heat of adsorption of triethylamine on Al_2O_3/SiO_2 at 473 K is shown in Fig. 2. The initial differential heat of triethylamine adsorption on Al_2O_3/SiO_2 at 473 K is calculated as 261 kJ mol^{-1}. At 423 K the initial differential heat of adsorption was 223 kJ mol^{-1}. A comparison of the results at 423 and 473 K shows that the adsorption at 423 K was nonspecific giving average values. The integral heat data at 423 K cannot be fitted adequately with the Langmuir model when the monolayer coverages for sites 1 and 2 are kept close to the values found for pyridine. However, if we only use the more certain results at low coverages and fix the monolayer coverages for sites 1 and 2 at the values used for ammonia and fix the parameters for site 3 to those found on silica, then an estimate of the re-

maining parameters can be obtained. The parameters found in this manner are given in Table 2.

All the parameters determined are within the range of realistic limits. The entropy change of adsorption for site 1 represents approximately a 98% loss of the gas phase entropy indicating irreversible adsorption. The entropy change for site 2 represents about 54% of the gas phase entropy, and although it probably corresponds to immobile adsorption, there is still a significant fraction of the rotational entropy available. The fitted heat determined for site 1 is considerably higher than the initial differential heat determined experimentally suggesting that even at 473 K this strong base gives average values at low coverages and the distribution of acid sites is less certain.

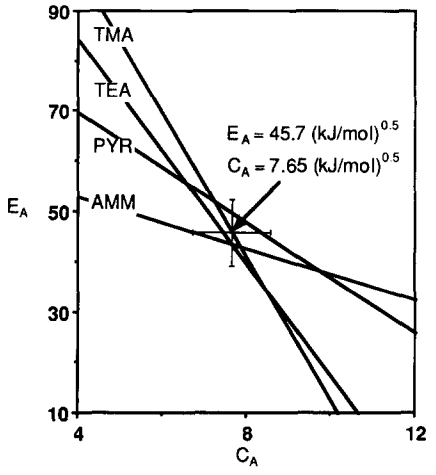

FIG. 4. Graphical representation of the determination of Drago–Wayland parameters for Al_2O_3/SiO_2 determined using the initial differential heat of adsorption.

Determination of Drago–Wayland Acid–Base Parameters and Discussion of Results of Basic Probe Molecules

The results presented above demonstrate that the differential heat of adsorption is strongly dependent on the base adsorbed. Therefore, when attempting to establish an acidity scale, the results must be compared with respect to a given probe molecule. The applicability of this approach for the prediction of new properties is one-dimensional. One can only predict the differential heat of adsorption of the defining probe molecule on a new catalyst if this catalyst is similar to those studied in the correlation. A more general approach would allow the prediction of thermodynamic properties of adsorption on a catalyst of other molecules of interest, like reactants and products for a given reaction. Such a correlation could be used to predict the thermodynamic behavior of both new catalysts and the molecules adsorbed on those new catalysts. Knowledge of these properties would be of help for the design of new catalytic processes. Here we test the viability of the prediction of heats of interaction of molecules with oxide surfaces via the Drago–Wayland theory and thermodynamic properties of the adsorptives.

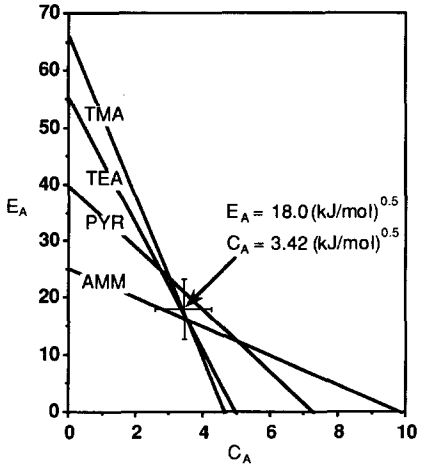

FIG. 3. Graphical representation of the determination of Drago–Wayland parameters for silica.

Using the procedure described in Ref. (*1*, *22*), we can estimate E_A and C_A parameters for silica and for different regions of Al_2O_3/SiO_2. Thus, by fitting the calorimetric results with Eq. (1) we obtained estimates for adsorption at low coverages on Al_2O_3/SiO_2, adsorption on sites 1 and 2 determined with the Langmuir model, and adsorption on silica. The parameters with their standard er-

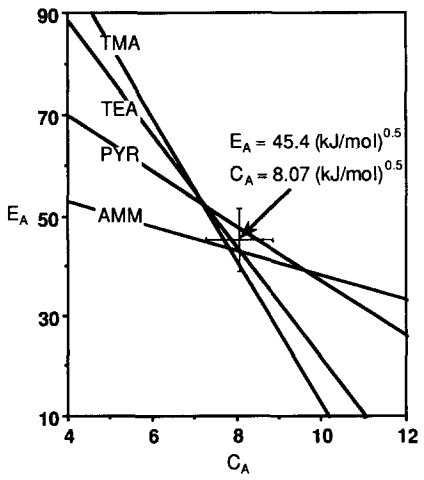

FIG. 5. Graphical representation of the determination of Drago–Wayland parameters for Al_2O_3/SiO_2 determined using the fitted differential heat of adsorption for site 1.

rors are summarized in Table 3. To illustrate the adequacy of the fit, representative graphical plots of the results are provided in Figs. 3–5 with 95% confidence intervals.

Adequate fits were obtained for all the heats except for those determined for site 2 on Al_2O_3/SiO_2 as seen in Table 3. This was expected because we were unable to identify accurately an intermediate step in the differential heat plots for the adsorption of ammonia, trimethylamine, and triethylamine on Al_2O_3/SiO_2. It appears that the adsorption of these molecules was not specific at the conditions used or that we did not have sufficient resolution to observe such a step. Since we were able to obtain reasonable agreement with the experimental data when the integral heat was fitted with constrained monolayer coverages corresponding to those found for pyridine, it seems that the nonspecific hypothesis is the more appropriate explanation.

The Drago–Wayland equation describes accurately the heats of interaction on Al_2O_3/SiO_2 at low and high coverages. As discussed in our previous work (1, 2), the initial heats of adsorption correspond to the interaction of the bases with the strongest Lewis sites on Al_2O_3/SiO_2 and this is a good quantity to characterize the acid strength of a catalyst. The large magnitude of E_A for the initial heat, which respresents the electrostatic contribution to the interaction, is consistent with adsorption on Lewis acid sites. The electrostatic contribution to the bond is about six times larger than the covalent contribution. The same ratio is observed for adsorption on silica, but the magnitude of the parameters is approximately 40% of the values determined for Al_2O_3/SiO_2.

The proton affinity of a species is a measure of its inherent gas phase basicity (*32*). An increase in the proton affinity of the base should produce a corresponding increase in the heat of interaction with a given acid. This is observed experimentally as shown in Fig. 6. A good correlation is found for both silica and Al_2O_3/SiO_2. Presumably a similar correlation could be found for other types of acid sites, giving another approach for acid strength prediction.

The ionization potential of a molecule is the amount of energy required to remove an electron from the molecule (*32*). As such it is a measure of the tendency of a molecule

TABLE 3
Summary of Drago–Wayland Parameters for SiO_2 and Al/SiO_2

Acid site	E_A (kJ mol^{-1})$^{1/2}$	Standard error (kJ mol^{-1})$^{1/2}$	C_A (kJ mol^{-1})$^{1/2}$	Standard error (kJ mol^{-1})$^{1/2}$
q_{init}SA	45.7	2.4	7.65	0.33
q_1SA	45.3	2.3	8.07	0.28
q_2SA	31.1	12.6	5.06	1.58
qSiO$_2$	18.0	1.9	3.42	0.30

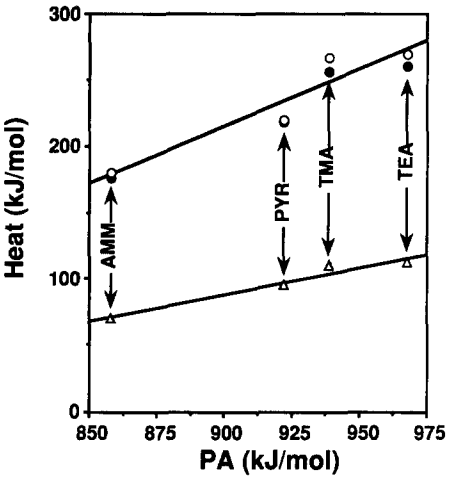

FIG. 6. Differential heats of adsorption on Al_2O_3/SiO_2 and on SiO_2 as a function of the proton affinity of the base (●, Al_2O_3/SiO_2 initial heat; ○, q_1 for Al_2O_3/SiO_2 from Langmuir model fit; △, SiO_2).

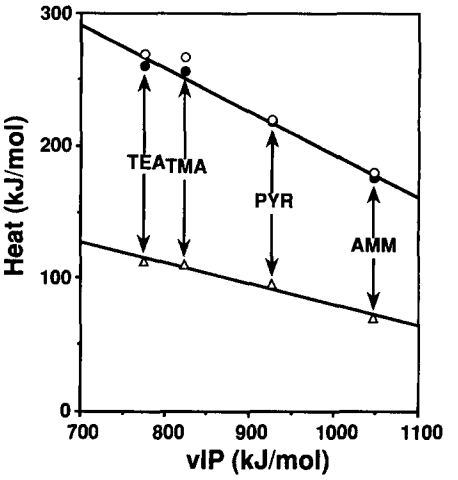

FIG. 7. Differential heats of adsorption on Al_2O_3/SiO_2 and on SiO_2 as a function of the vertical ionization potential of the base (●, Al_2O_3/SiO_2 initial heat; ○, q_1 for Al_2O_3/SiO_2 from Langmuir model fit; △, SiO_2).

to donate electrons. A Lewis acid–base interaction involves the donation of electrons from the base to acid. Thus a decrease in the ionization potential of a species corresponds to an increase in basic strength and should produce a stronger interaction with a given acid. Once again this is confirmed experimentally for our samples, as illustrated in Fig. 7 with a nearly linear correlation.

The pK_a of the base, on the other hand, should not necessarily correlate with the gas phase basicity, because variation in the heats of solvation of the cationic conjugate acids of the bases in solution can produce basic strength reversals when compared with gas phase basicities (*33*). This is observed for ammonia and pyridine adsorption on our samples, as depicted in Fig. 8. Thus, the acid–base interactions taking place on the surface of silica and silica-supported alumina are apparently described better in terms of gas phase acid–base interactions than in terms of those interactions taking place in aqueous solutions. This is a reasonable result in view of the low water surface concentration of the samples in this study, which were pretreated at elevated temperatures prior to study. Barteau and Madix (*34*) observed a similar behavior for the relative acidities of a series of Brønsted acids adsorbed on Ag(110). The acidity scale obtained in that study was in agreement with the acidity scale for the species in the gas phase, but it could not be explained by the aqueous dissociation constants.

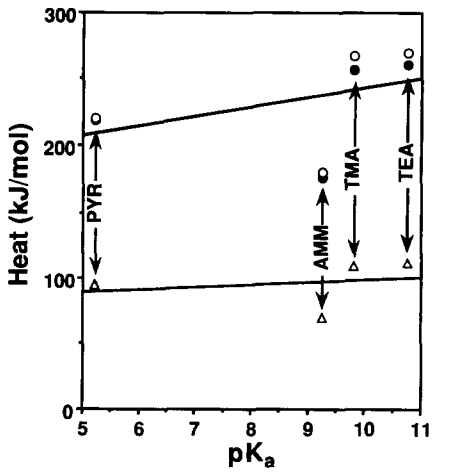

FIG. 8. Differential heats of adsorption on Al_2O_3/SiO_2 and on SiO_2 as a function of the pK_a of the base (●, Al_2O_3/SiO_2 initial heat; ○, q_1 for Al_2O_3/SiO_2 from Langmuir model fit; △, SiO_2).

CONCLUSIONS

The differential heats of adsorption of ammonia, trimethylamine, and triethylamine on silica–alumina and silica can be correlated using the Drago–Wayland theory. Accordingly, the surface acidic properties can be described in terms of a pair of parameters representing electrostatic and covalent interactions involved in the adsorption of basic molecules. Since such parameters are tabulated in the literature for many basic molecules, the Drago–Wayland parameters for surface acid sites could allow the prediction of heats of adsorption for a wide range of basic molecules. This is an area in which future research seems promising.

ACKNOWLEDGMENTS

We acknowledge the support of a National Science Foundation Equipment Grant that allowed us to purchase the microcalorimeter used in this work. Furthermore, we thank the Department of Energy for the partial financial support of this work (DE-FG02-84ER13183). Finally, we thank the Graduate Professional Opportunity Program and the Chevron Corporation for financial support for one of us (N.C.M.) during different stages of this work and the University of Puerto Rico–Mayagüez for providing a leave of absence to the same author.

REFERENCES

1. Cardona-Martínez, N., and Dumesic, J. A., *J. Catal.* **125,** 427 (1900).
2. Cardona-Martínez, N., and Dumesic, J. A., *J. Catal.* **127,** 706 (1991).
3. Drago, R. S., and Wayland, B. B., *J. Amer. Chem. Soc.* **87,** 3571 (1965).
4. Drago, R. S. *Struc. Bonding* **15,** 73 (1973).
5. Drago, R. S., Wong, N., Bigrien, C., and Vogel, G. C., *Inorg. Chem.* **26,** 9 (1987).
6. Joslin, S. T., and Fowkes, F. M., *Ind. Eng. Chem. Prod. Res. Dev.* **24,** 369 (1985).
7. Fowkes, F. M., McCarthy, D. C., and Tischler, D. O., *Polym. Sci. Technol.* **27,** 401 (1983).
8. Fowkes, F. M., *Rubber Chem. Technol.* **57,** 328 (1984).
9. Fowkes, F. M., *in* "Physicochemical Aspects of Polymer Surface" (K. L. Mittal, Ed.), p. 583, Vol. 2. Plenum, New York, 1981.
10. Lim, Y. Y., Drago, R. S., Babich, M. V., Wong, N., and Doan, P. E., *J. Amer. Chem. Soc.* **109,** 169 (1987).
11. Masuda, T., Taniguchi, H., Tsutsumi, K., and Takahashi, H., *Bull. Chem. Soc. Japan* **51,** 1965 (1978).
12. Masuda, T., Taniguchi, H., Tsutsumi, K., and Takahashi, H., *J. Japan Petrol. Inst.* **22,** 67 (1979).
13. Tsutsumi, K., Mitani, Y., and Takahashi, H., *Bull. Chem. Soc. Japan* **56,** 1912 (1983).
14. Auroux, A., and Védrine, J. C., *in* "Catalysis by Acids and Bases," p. 311, Elsevier, Amsterdam, 1985.
15. Kusnetsov, B. V., and Derkaui, A., *Zh. Fiz. Khim.* **57,** 1314 (1983).
16. Derkaui, A., Kiselev, A. V., and Kuznetsov, B. V., *Zh. Fiz. Khim.* **59,** 159 (1985).
17. Curthoys, G., Davydov, V. Ya., Kiselev, A. V., Kiselev, S. A., and Kuznetsov, B. V., *J. Colloid Interface Sci.* **48,** 58 (1974).
18. Masuda, T., Taniguchi, H., Tsutsumi, K., and Takahashi, H., *Bull. Chem. Soc. Japan* **51,** 633 (1978).
19. Masuda, T., Taniguchi, H., Tsutsumi, K., and Takahashi, H., *Bull. Chem. Soc. Japan* **52,** 2849 (1979).
20. Taniguchi, H., Masuda, T., Tsutsumi, K., and Takahashi, H., *Bull. Chem. Soc. Japan* **53,** 362 (1980).
21. Taniguchi, H., Masuda, T., Tsutsumi, K., and Takahashi, H., *Bull. Chem. Soc. Japan* **53,** 2463 (1980).
22. Cardona-Martínez, N., Ph.D. thesis, University of Wisconsin–Madison, 1989.
23. Dean, J. A., "Langes's Handbook of Chemistry," 12 ed. McGraw–Hill, New York, 1979.
24. Braker, W., and Mossman, A. L., "Matheson Gas Data Book," 6th ed., 1980.
25. Reid, R. C., Prausnitz, J. M., and Poling, B. E., "The Properties of Gases and Liquids." McGraw–Hill, New York, 1987.
26. Gay, I. D., and Liang, S., *J. Catal.* **44,** 306 (1976).
27. Knözinger, H., *Adv. Catal.* **25,** 184 (1976).
28. Wollrab, J. E., and Laurie, V. W., *J. Chem. Phys.* **51,** 1580 (1969).
29. Gayles, J. N., *Spectrochim. Acta A* **23,** 1521 (1967).
30. Fleischman, S. H., Weltin, E. E., and Bushweller, C. H., *J. Comput. Chem.* **6,** 249 (1985).
31. Cramer, R. E., and Bopp, T. T., *J. Chem. Educ.* **54,** 612 (1977).
32. Bartmess, J. E., and McIver, R. T., Jr., *in* "Gas Phase Ion Chemistry" (M. T. Bowers, Ed.), Vol. 2. Academic Press, New York, 1979.
33. Perrin, D. D. *in* "Dissociation Constants of Organic Bases in Aqueous Solution: Supplement 1972." Butterworths, London, 1972.
34. Barteau, M. A., and Madix, R. J. *Surf. Sci.* **120,** 262 (1982).